Carbohydrate Polymers 84 (2011) 1192–1200

Contents lists available at ScienceDirect

Carbohydrate Polymers

journal homepage: www.elsevier.com/locate/carbpol

Preparation and characterizations of a novel deoxycholic acid–O-carboxymethylated chitosan–folic acid conjugates and self-aggregates

Feihu Wang[a], Dianrui Zhang[a,*], Cunxian Duan[a], Lejiao Jia[a], Feifei Feng[a], Yue Liu[a], Yancai Wang[a], Leilei Hao[a], Qiang Zhang[b]

[a] Department of Pharmaceutics, College of Pharmacy, Shandong University, 44 Wenhua Xilu, Jinan 250012, PR China
[b] State Key Laboratory of Natural and Biomimetic Drugs, School of Pharmaceutical Sciences, Peking University, 38 Bei Xueyuan Road, Beijing 100083, PR China

ARTICLE INFO

Article history:
Received 4 October 2010
Received in revised form 9 January 2011
Accepted 12 January 2011
Available online 18 January 2011

Keywords:
O-carboxymethylated chitosan
Deoxycholic acid
Folic acid
Self-aggregates

ABSTRACT

O-carboxymethylated chitosan (OCMC) was firstly hydrophobically modified with various deoxycholic acid (DOCA) to obtain a novel kind of amphiphilic polymer, and then covalently bound with folic acid (FA) to develop a new potential cancer-targeted drug delivery system. Structural characterizations of the conjugates were investigated using FTIR, ^{1}H NMR and XRD. The physicochemical properties of self-aggregates in aqueous media were studied by ^{1}H NMR, zetasizer, zeta potential, fluorescence spectroscopy, and transmission electron microscopy (TEM). The mean diameter of self-aggregates in PBS solution (pH 7.4) decreased with the degree of substitution (DS) of DOCA increasing. Zeta potential of self-aggregates exhibited near −20 mV in PBS solution (pH 7.4), indicating these nanoparticles were covered with negatively charged OCMC shells. The critical aggregation concentrations (cac) of the conjugates were dependent on the DS of DOCA and were significantly lower than those of low molecular weight surfactants. TEM images demonstrated that the shape of self-aggregates was spherical.

1. Introduction

Recently, amphiphilic polymers consisting of hydrophilic and hydrophobic moieties have received increasing interest because of their potential biotechnological and pharmaceutical applications (Gref et al., 1994; Kataoka, Harada, & Nagasaki, 2001; Tobio, Gref, Sanchez, Langer, & Alonso, 1998). In an isotropic aqueous solution, various amphiphilic polymers spontaneously form micelles or self-aggregates which are promoted by intra- and/or intermolecular association between hydrophobic segments, primarily to minimize interfacial free energy (Akiyoshi, Deguchi, Moriguchi, Yamaguchi, & Sunamoto, 1993; Kataoka et al., 2001; Mortensen, 2001; Nagasaki, Yasugi, Yamamoto, Harada, & Kataoka, 2001). These polymeric micelles or self-aggregates consist of the inner core of hydrophobic segments and the outer shell of hydrophilic segments, and this core–shell structure has been recognized as a promising delivery carrier because the hydrophobic core can serve as a reservoir for various hydrophobic bioactive agents (Kataoka, Kwon, Yokoyama, Okano, & Sakurai, 1993; Kataoka et al., 2001; Nagasaki et al., 2001). Also, these polymeric micelles exhibit the unique characteristics, such as unusual rheological feature, small hydrodynamic radius, and thermodynamic stability (Huh et al., 2000; Kakizawa, Harada, & Kataoka, 2001; Tae, Kornfield, Hubbell, & Lal, 2002). Therefore, in the past decades, many efforts have been made to develop some novel amphiphilic polymers such as amphiphilic block copolymers (Kabanov et al., 1995; Lee et al., 1999; Nagasaki et al., 2001; Poppe, Willner, Allgaier, Stellbrink, & Richter, 1997) and hydrophobically modified polymers (Huh et al., 2000; Kim et al., 2000) which form compact micellar structure in an aqueous media self-assembly. In recent years, much attention has been paid to natural polysaccharides, such as chitosan, dextran and pullulan, which can been hydrophobically modified with alkyl chains and bile acids to form nanosized micelles or self-aggregates as drug delivery systems (Akiyoshi et al., 2000; Kuroda, Fujimoto, Sunamoto, & Akiyoshi, 2002; Na & Bae, 2002; Yuan, Li, Zhu, & Woo, 2006). In particular, self-aggregates of hydrophobically modified chitosan are formed in an aqueous solution, showing as a promising potential carrier for hydrophobic drugs and genes (Kim et al., 2001; Kwon et al., 2003; Yuan, Li, & Yuan, 2006).

Chitosan, the *N*-deacetylated derivative of chitin, is a copolymer of glucosamine and N-acetyl-D-glucosamine linked together by β(1,4) glycosidic bonds. Recently, researchers concentrated on chitosan as a drug (Lee, Kim, Kwon, & Jeong, 2000; Ruel-Gariepy, Leclair, Hildgen, Gupta, & Leroux, 2002; Zhang & Zhang, 2002) or gene (Kim et al., 2001; Koping-Hoggard et al., 2001; Lee, Kwon, Kim, Jo, & Jeong, 1998) carrier because of its biocompatibility,

* Corresponding author. Tel.: +86 531 88382015; fax: +86 531 88382015.
E-mail address: zhangdianrui2006@163.com (D. Zhang).

0144-8617/$ – see front matter.
doi:10.1016/j.carbpol.2011.01.017

biodegradability, low toxicity and good availability. However, the poor solubility of chitosan in biological solution (pH 7.4) is a major drawback for its extended application in drug delivery systems. It was reported that, the water solubility of chitosan could be advanced by various approaches such as quaternization of the amino group, carboxymethylation, and pegylation. Glycol modified chitosan with a stable nanoparticle structure in physiological conditions show a good water solubility and biocompatibility (Kwon et al., 2003; Park et al., 2004; Son et al., 2003). Carboxymethylation is considered as a method to improve the water solubility for many polysaccharides. O-carboxymethylated chitosan (OCMC), a kind of carboxymethylated derivative of chitosan, contains –COOH and $-NH_2$ groups in the molecular structure and is prepared by chemical reactions of chitosan and monochloroacetic acid. The good biocompatibility, bioactivity, antibacterial activity, stability and aqueous solution property of OCMC have been reported in some early papers (Chen & Park, 2003; Chen, Du, Tian, & Sun, 2005; Liu, Guan, Yang, Li, & Yao, 2001). Deoxycholic acid (DOCA), a main component of bile acid, contains the hydrophilic moieties such as the carboxyl group at the end of the branched side chain of carbon atoms and the hydroxyl groups at both 3α and 12α positions and the hydrophobic cyclopentenophenanthrene nucleus in its molecule. DOCA can form micelles in water because of its amphiphilicity, which plays an important role in the emulsification, solubilization, and absorption of cholesterol, fat, and vitamins in the body (Enhsen, Kramer, & Wess, 1998). Thus, it was expected that the introduction of DOCA into the OCMC would induce self-association to form self-aggregates.

However, this kind of self-aggregates could not escape from the reticuloendothelial system (RES), and would be scavenged by the mononuclear phagocyte system (MPS). Moreover, the inadequate uptake of the self-aggregates at tumor sites will decrease the effect of the administered drug dose, and non-specific accumulation in healthy tissues can lead to toxic side effects, limiting the maximum dosage that can be safely used. These constraints prevent drug-loaded self-aggregates from achieving the potential therapeutic effect which might otherwise be attained (Han et al., 2009). To achieve cancer-targeted drug delivery, several methods have been attempted, one strategy is the utilization of unique molecular markers that are specifically overexpressed within the cancerous tissues. It is well known that folate receptor (FR), folate-binding protein, is overexpressed on the surface of many human epithelial cancer cells, including cancers of the ovary, kidney, uterus, colon, and lung, but rarely found on normal cell surface (Liu, Wiradharma, Gao, Tong, & Yang, 2007; Lu & Low, 2003; Zhang, Kohler, & Zhang, 2002). Folic acid (FA) is appealing as a ligand because it is useful for targeting cell membranes and enhancing endocytosis of nanoparticles via the FRs (Chan, Kurisawa, Chung, & Yang, 2007; Park, Lee, & Lee, 2005). Importantly, FA conjugates, which are covalently derivative via its γ-carboxyl group, can retain a strong affinity toward its receptor, and the mechanism of cellular uptake of FA conjugates by FRs is similar to that of FA chemicals (Chan et al., 2007). Recycling of FRs in target cells can lead to transporting more FA conjugates (Wang et al., 1997). So far, many researches have been reported on FA conjugated polymeric micelles, macromolecules, nanoparticles and liposomes for the targeted delivery of anticancer agents or genes (Lee & Low, 1994; Lee, Na, & Bae, 2003; Mansouri, Cuie, Winnik, Shi, & Lavigne, 2006; Oyewumi, Yokel, Jay, Coakley, & Mumper, 2004; Zhao, Yue, & Lanry, 2008).

In our study, OCMC was firstly hydrophobically modified with DOCA, then covalently bound with FA to develop a new cancer-targeted drug delivery system. Herein, we investigated the effects of degree of substitution (DS) and pH of the medium on the formation of self-aggregates in detail, and the physicochemical characteristics of self-aggregates in aqueous media were also studied.

2. Materials and methods

2.1. Materials

OCMC ($M_n = 8.5 \times 10^4$, degree of deacetylation = 90%, degree of carboxymethylation = 85%) was purchased from Hong Hai Biotechnology Co., Ltd. Qingdao (China). DOCA, FA, 1-ethyl-3-(3-dimethylaminopropyl)-carbodiimide hydrochloride (EDC), and pyrene were obtained from Sigma Co. (USA). *N*-Hydroxy succinimide (NHS) was purchased from Alfa Aesar (USA). All reagents were analytical grades and used without further purification. Water was purified by distillation, deionization, and reverse osmosis (Milli-Q plus) .

2.2. Modification of OCMC with DOCA

The course of reaction was shown in Scheme 1a. The OCMC (0.25 g) was dissolved in distilled water (25 mL), followed by dilution with methanol (75 mL). Different amounts of activated DOCA (0.0115–0.345 mol/mol sugar residues of OCMC) were added and stirred until the solutions were optically transparent. To activate the carboxylic acid groups of DOCA in dried DMSO, equal amounts (1.5 equiv./DOCA) of EDC and NHS were added into the solution, which allowing the formation of an amide linkage by the reaction with primary amino groups in OCMC. The resulting solution reacted by stirring for 36 h at room temperature. Then, the reactant mixture was dialyzed against the excess amount of water/methanol mixture (1 v/4 v) for 3 days using a dialysis tube (molecular cut off 12,000), followed by lyophilization to obtain DOMC conjugates.

2.3. Synthesis of DOMC–FA conjugates

Folate was attached to the surface amino groups of DOMC via a carbodiimide reaction as described by Mansouri et al. (2006) and Yang et al. (2010) (Scheme 1b). Briefly, FA (0.25 or 0. 5 mol/mol sugar residues of DOMC) was dissolved into a mixture of anhydrous DMSO (5 mL) and triethylamine (TEA, 0.5 mL), and activated by equal amounts (2 equiv./FA) of EDC and NHS under nitrogen anhydrous conditions for 2 h at room temperature. The DOMC (0.25 g) was dissolved in distilled water (25 mL), followed by dilution with methanol (25 mL). Stirred until the solutions were optically transparent, then activated FA was added dropwise to DOMC solution. The resulting mixture was stirred at room temperature for about 24 h under nitrogen atmosphere to let FA conjugate onto chitosan molecules, and then titrated to pH 9.0 with 0.1 M NaOH to terminate the reaction. The solution was dialyzed first against phosphate buffer (PBS, pH = 7.4) for 3 days to remove excess of unreacted substrates and then against distilled water for 3 days. The polymer was isolated by lyophilization. The final product DOMC–FA was a yellow dry powder and the purity quotient was detected by HPLC analysis (Agilent 1100 Series, USA). All the processes were operated in the dark.

2.4. Characterization of the polymers

The chemical structures of OCMC and DOMC conjugates were analyzed using a Fourier transform infrared (FT-IR) spectrophotometer (KBr pellets, BRUKER VERTEX70, Germany) and ^{1}H NMR spectra of the OCMC, DOMC and DOMC–FA were measured in D_2O or D_2O/DMSO-d6 (3:1, v/v) using a 600 MHz spectrometer (Inova-600, Varian, USA).

X-ray diffraction (XRD) spectrometry was obtained using an XD-3A powder diffractometer (D/Max r-B, Rigaku, Japan). A Cu Kα radiation at 40 kV and 100 mA was used. Diffractograms were performed from the initial angle $2\theta = 3^\circ$ to the final angle $2\theta = 50^\circ$ with the steps of 0.02°, at a scanning speed of 4°/min (2θ).

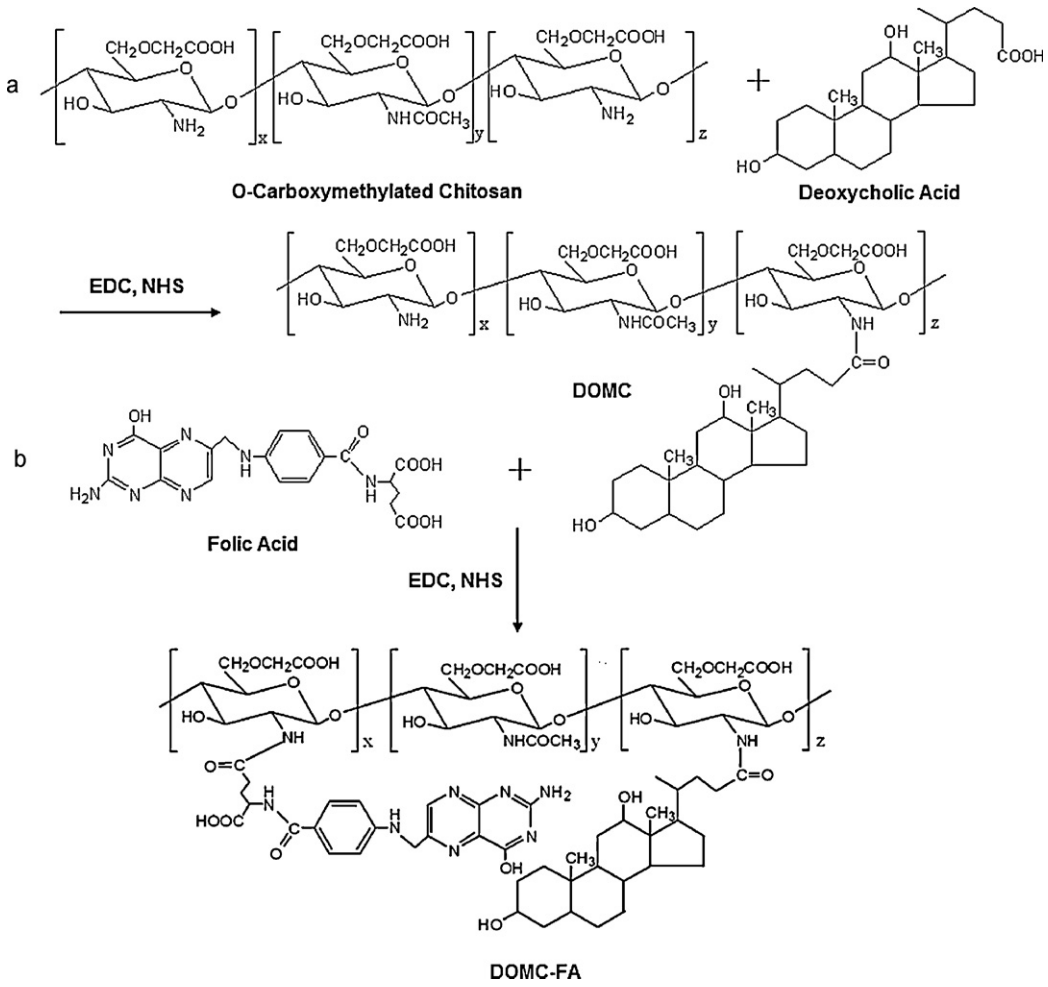

Scheme 1. The modification process of OCMC.

2.5. Determination of degree of substitution

2.5.1. DOCA content

The amount of DOCA covalently bounded to OCMC was determined spectrophotometrically according to the procedure described by Yuan, Li, and Yuan (2006), Nichifor and Carpov (1999). Briefly, the polymer sample (4–10 mg) was accurately weighed in an ampoule and dissolved in 0.5 mL DMSO, then 0.5 mL 60% aqueous acetic acid solution and 9.0 mL water/sulfuric acid (65/50, v/v) were successively added. The content of the ampoule was homogenized, heated at 70 °C for 30 min, then cooled to room temperature. The UV (UV-2102PCS, UNICO, Shanghai, China) absorbance at 378 nm was measured against a blank containing the same components as the sample but without the polymer. Individual calibration curves of absorbance versus DOCA concentrations were made. The degree of substitution (DS, mol%, expressed as mole DOCA/100 sugar residues of OCMC) was calculated according to the following formula:

$$\mathrm{DS} = \frac{c/M_{\mathrm{DOCA}}}{(m-c)/M_{\mathrm{OCMC}}}$$

where c is the content of the DOCA determined from the corresponding calibration curve; m is the amount of the modified polymers used in experiment; M_{DOCA} is the molecular weight of the DOCA residue; M_{OCMC} is the molecular weight of units OCMC units (Ugl). The DS values were also determined from ^{1}H NMR spectra (Yuan, Li, & Yuan, 2006).

2.5.2. FA content

The molar ratios of FA to amino groups in final conjugates were determined by a UV/vis spectrophotometer using the molar extinction coefficient value of 6197 mol^{-1} cm^{-1} at λ = 363 nm (Reddy & Low, 1998). Briefly, accurately weighed folate derivative was dissolved in water and DMSO (1/1, v/v) to obtain a 0.02 wt.% DOMC–FA conjugate solution, and then measured with UV/vis spectrophotometer. FA powder was dissolved and diluted to a series of gradient FA standard solutions that were used to prepare the calibration curve in the range of 5–35 μg/mL for further analysis. The degree of substitution (DS), defined as the number of FA per 100 sugar residues of OCMC was calculated according to the following formula:

$$\mathrm{DS} = \frac{c/M_{\mathrm{FA}}}{(m-c-m1)/M_{\mathrm{OCMC}}}$$

where c is the content of the FA determined from the corresponding calibration curve; m is the amount of the modified polymers used in experiment; m_1 is the amount of the DOCA contained in the modified polymers used in experiment; M_{FA} is the molecular weight of the FA; M_{OCMC} is the molecular weight of OCMC units (Ugl).

2.6. Preparation of self-aggregates

The DOMC and DOMC–FA conjugates were suspended in various pH phosphate-buffered saline (PBS) solution (identical ionic strength = 0.2) under gentle shaking at room temperature for 8 h.

The solution was then sonicated three times using a probe-type sonifier (JY92-IIUltrasonic Processor, Xinzhi, Linbo, China) at 90 W for 2 min each, in which the pulse was turned off for 2 s with the interval of 4 s to prevent the increase of temperature. Then, the solution of self-aggregates was passed through membrane filter (pore size: 0.45 μm, Millipore) and stored at 4 °C in refrigerator.

2.7. Evaluation of particle size and zeta potential

The average particle size and size distribution of self-aggregates were determined using a Zetasizer (3000HS, Malvern Instruments Ltd, UK).

The zeta potentials of self-aggregates were measured with a zeta potential analyzer (Brookhaven ZetaPALS, USA). The concentration of self-aggregates was kept constant at 2.0 mg/mL in PBS solution.

2.8. Measurement of fluorescence spectroscopy (pyrene)

To investigate the fluorescence spectroscopy characteristics, the DOMC and DOMC–FA suspensions were prepared by the same procedure as mentioned for preparation of the aggregates above. The potential of self-aggregates property and the critical aggregation concentration (CAC) of the DOMC and DOMC–FA conjugates were estimated by the probe fluorescence technique (Gao et al., 2008), using pyrene as a hydrophobic probe. Briefly, a certain amount of pyrene solutions (3×10^{-4} M) in acetone were added to a series of vials, and followed by evaporation to remove the acetone. Then, various conjugates suspensions, of which concentration ranged from 1.0×10^{-4} to 2.0 mg/mL, were added to each vial and sonicated in an ultrasonic bath (KQ3200E, China) for 3 h to equilibrate the pyrene and the nanoparticles, and then left undisturbed to cool overnight at room temperature. The final concentration of pyrene in each sample was 6.0×10^{-7} M. To obtain pyrene emission spectra, the slit widths for excitation and emission were set at 5 and 2.5 nm, respectively. The emission spectra of pyrene were performed at a range from 350 to 500 nm using a fluorescence spectrophotometer (F-2500, Hitachi, Japan) at the excitation wavelength of 334 nm and an integration time of 4 s/nm.

2.9. Transmission electron microscopy (TEM) observation

The morphology and size of self-aggregates were observed using a transmission electron microscope (TEM) (H-7000, Hitachi, Japan). A drop of sample solution (2 mg/mL) was placed onto a 300-mesh copper grid coated with carbon. After 2 min, the grid was tapped with a filter paper to remove surface water, followed by air drying and negatively stained with 2% phosphotungstic acid for 30 s. The grid was dried at room temperature and then observed by TEM.

3. Results and discussion

3.1. Synthesis and characterization of DOMC and DOMC–FA conjugates

For the synthesis of DOMC and DOMC–FA conjugates, EDC and NHS reacted with a carboxyl group of the DOCA and FA, respectively, to initially form an active ester intermediate, which covalently attached to a primary amine group of the OCMC to form an amide bond, thus producing a novel kind of targeted amphiphilic polymer. In the FT-IR spectra (data not shown), the characteristic absorption bands of OCMC appeared at 1597 cm^{-1}, assigned to the N–H bending vibration of the primary amine group, which covered the amide I and II band and showed the high degree of deacetylation of OCMC. For the DOMC spectrum, compared with natived OCMC, the absorption band at 1601 cm^{-1} was evidently decreased, and there were two new absorption peaks for the C=O group. The peak at about 1635 cm^{-1} was ascribed to the amide I band stretching vibration and the peak at about 1726 cm^{-1} was due to the carboxyl characteristic peaks in protonated form (Sandula, Kogan, Kacurakova, & Machova, 1999). These results are evidence of the conjugation of DOCA onto OCMC by acylation of amide linkages. Also, the presence of DOCA in DOMC was verified by the characteristic peaks of DOCA appearing at 0.5–2.5 ppm in the ^{1}H NMR spectra (Kim et al., 2005). As shown in Fig. 1, compared with the spectrum of OCMC (Fig. 1a) and DOCA (Fig. 1b), the signals of DOCA in DOMC (Fig. 1d) at 0.53, 0.74, 0.77 and 0.78 ppm were correspond to the protons of CH_3 groups at positions 18, 19 and 21 of the steroid skeleton of DOCA, respectively (Yuan, Li, & Yuan, 2006).

Successful synthesis of the folate residue with DOCA grafted OCMC was confirmed by a ^{1}H NMR spectroscopy. Compared with the ^{1}H NMR spectra of DOMC and FA (Fig. 1e), the appearance of signals at 6.5–9.0 ppm in the ^{1}H NMR spectrum of DOMC–FA (Fig. 1f) is attributed to the resonance of the folate aromatic protons. The signal at 8.58 ppm is corresponded to the proton at the 7-position of the pterin ring of FA, and for the signals at 7.56 and 6.71 ppm which are due to the FA proton from the H13/15 and H12/16, respectively (Wan, Sun, & Li, 2008). They revealed the couple of the folate residue to the DOMC. Also, the singles of DOCA were observed in DOMC–FA conjugates, that is to say, there are DOCA molecules in both DOMC and DOMC–FA conjugates.

By this coupling reaction, various DOMC conjugates with different DS of DOCA were prepared by controlling the feed ratio of DOCA to OCMC. The DS is in the range from 3.6 to 6.9 per 100 sugar residues of OCMC in this experiment, and good agreement of the results obtained by the two methods (UV and NMR) were observed. The relevant signals of folate were much weaker than the broad and strong proton signals of DOCA and OCMC residues. Therefore, for more accurate evaluation, the DS of folate was assessed by UV spectroscopy as described in Section 2. The grafting degrees of DOCA of DOMC and folate of DOMC–FA are listed in Table 1.

In order to investigate the changes of the microstructure between OCMC and its derivative, X-ray diffraction experiments were performed. The X-ray diffraction patterns of the OCMC (a), DOCA (b), DOMC7 (c), FA (d) and DOMC–FA2 (e) are displayed in Fig. 2. Native OCMC had diffraction at $2\theta = 20.5°$ and $2\theta = 22.4°$ which was assigned to the crystal form. The diffraction curve of DOCA exhibited a sharp peak at 2θ equals 10.8°, 13.5°, 14.1°, 15.0°, 16.1°, 17.9°and 19.1°, and FA had sharp peaks at 2θ equals 10.7°, 12.9°, 16.2°, 16.8°, 19.1°, 26.5°, 26.9° and 27.6°. In contrast to OCMC, the peak at $2\theta = 20.5°$ disappeared and the intensity and location of peaks were changed obviously in the diffraction pattern of DOMC7, indicating a less ordered structure and crystal defects. However, the DOMC–FA2 showed no sharp diffraction peaks at all and the intensity of peaks was much weaker. These results indicated that the crystalline structure of OCMC had been completely disrupted, proving DOCA and FA were coupled to OCMC.

In this experiment, the degree of deacetylation of OCMC was 90%. Although DOCA and OCMC were reacted by stirring for 36 h in solution, the maximum degree of substitution of DOCA was 6.9%. That is to say, there were still 83.1% of free amino groups on the surface of OCMC, which could conjugate with FA. The DS of FA increased with the increasing in the feed ratio of FA, which indicated that the DS of DOCA had no effect on FA coupled to OCMC.

3.2. Self-aggregation of DOMC and DOMC–FA conjugates

The DOMC, composed of hydrophilic OCMC and hydrophobic DOCA, was characterized using ^{1}H NMR in different solvent systems including both D_2O and D_2O/DMSO-d6 (3:1, v/v) (Fig. 1). For the ^{1}H NMR results in D_2O/DMSO-d6 (3:1, v/v) (Fig. 1d), an available

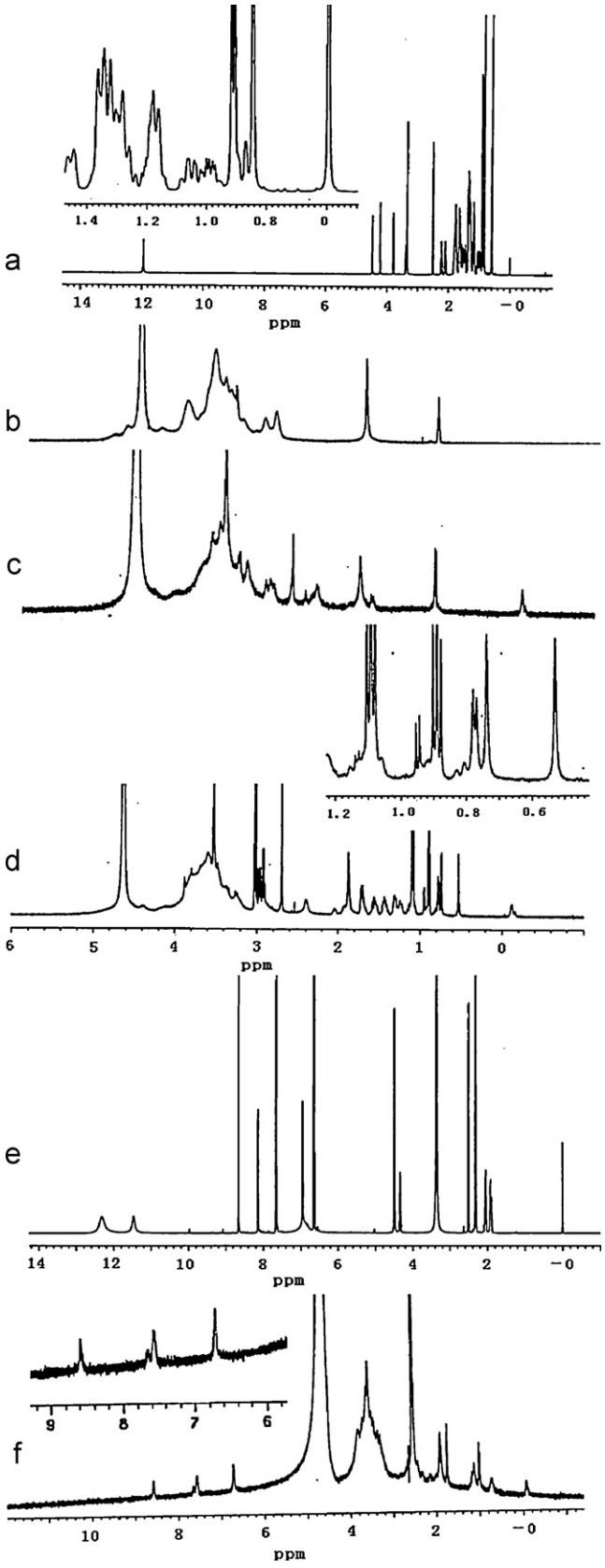

Fig. 1. ^{1}H NMR spectra of DOCA in DMSO-d6 (a), OCMC in D_2O (b), DOMC in D_2O (c), DOMC in D_2O/DMSO-d6 (3:1, v/v) (d), FA in DMSO-d6 (e) and DOMC–FA in D_2O/DMSO-d6 (3:1, v/v) (f) at 25 °C.

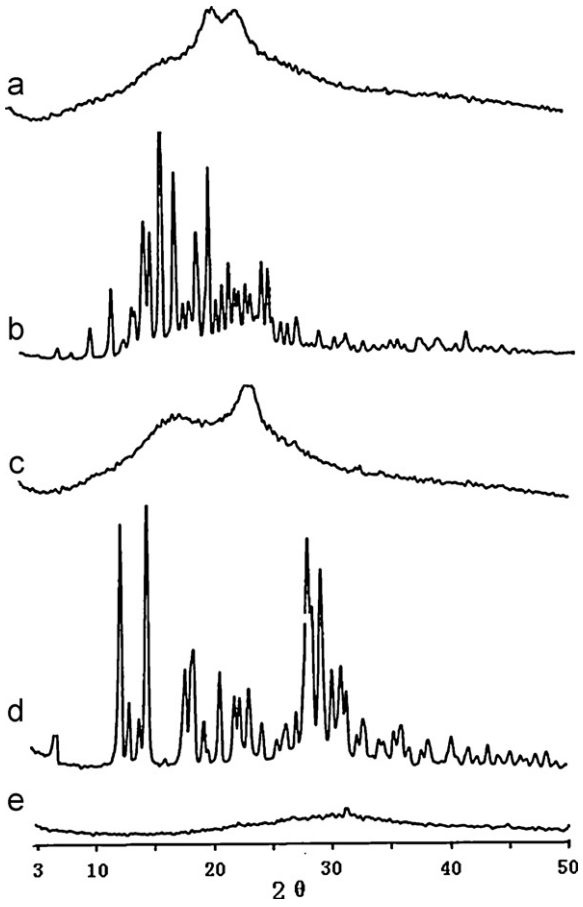

Fig. 2. WAXD spectra of OCMC (a), DOCA (b), DOMC7 (c), FA (d) and DOMC–FA2 (e). Results indicated that DOCA and FA coupled to OCMC.

solvent for dissolving both OCMC and DOCA, all the characteristic peaks of the DOMC conjugates were clearly observed, whereas the characteristic proton peaks of DOCA, including 18-CH_3, 19-CH_3, 21-CH_3 and methylene–methine, significantly decreased in D_2O (Fig. 1c). It indicated that the molecular motion of hydrophobic DOCA in DOMC was limited because of the formation of self-aggregates in D_2O, thus causing proton signal shielding or peak broadening of DOCA. This trend in the ^{1}H NMR spectra was consistent with other amphiphilic polymers that form micelles or nanoparticles in the aqueous phase (Kim et al., 2000; Kim, Lee, Kwon, Chung, & Jeong, 2002; Kwon et al., 2003). So, the

Table 1
Properties of DOCA hydrophobic-modified OCMC and FA conjugations in PBS solution (pH = 7.4).

Sample[a]	DS[b] (%)	X^c (%)	d^d (nm)	PI[d]	ξ^e (mV)	CAC[f] (mg/mL)
DOMC4	3.6	6.08	383.5	0.351	−17.03	0.0655
DOMC5	4.7	7.79	321.7	0.327	−16.53	0.0569
DOMC6	5.6	8.85	290.0	0.372	−16.27	0.0438
DOMC7	6.9	11.04	231.1	0.365	−16.23	0.0273
DOMC–FA1	6.8	11.04	212.5	0.259	−15.98	0.0257
DOMC–FA2	14.3	11.04	179.4	0.345	−15.22	0.0227

[a] In DOMC conjugates, where the number indicates the DS of DOCA; the DOMC–FA conjugates were produced by DOMC7 with different amounts of FA.
[b] Degree of substitution expressed as mole DOCA (in DOMC) and FA (in DOMC–FA) per 100 sugar residues of O-carboxymethylated citosan.
[c] Weight fraction of DOCA.
[d] Mean diameter and polydispersity indices measured by a Zetasizer.
[e] The ξ potential of the DOMC and DOMC–FA conjugated in PBS solution(pH = 7.4) at 2 mg/mL.
[f] Critical aggregation concentration determined by fluorescence spectroscopy.

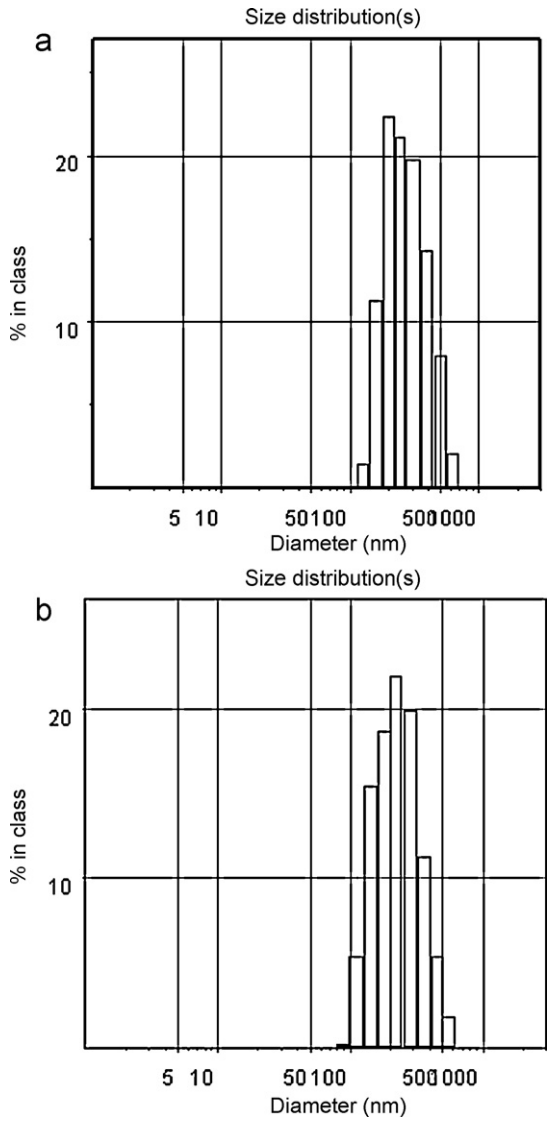

Fig. 3. Histograms of the size distribution of self-aggregated nanoparticles (DOMC7 (a) and DOMC–FA2 (b)). Compared with DOMC7, DOMC–FA2 has a narrow size distribution.

DOMC–FA conjugates, composed of the hydrophilic chain OCMC and hydrophobic segment DOCA, must self-aggregates in aqueous media to form core–shell structured nano-micelles. The micellar core was assembled by a hydrophobic effect of the DOCA, while the hydrophilic chain OCMC comprised the brush-like structured shell of the micelles, and FA, the targeting group, which dissolved in the medium was on the surface of the nano-micelles.

The size and size distribution of self-aggregates of DOMC and DOMC–FA conjugates with different DS in a PBS solution (pH = 7.4) were measured by a Zetasizer. As shown in Table 1, the mean sizes of self-aggregates of DOMC were in the range of 231–383 nm and DOMC–FA were slightly smaller with the size of 179–212 nm. Obviously, the size of self-aggregates decreased as the DS increased, indicating formation of more dense hydrophobic cores because of the enhanced hydrophobic interaction between DOCA attached to OCMC. The polydispersity indices (PI) of self-aggregates were relatively low (0.259–0.372), implying a narrow size distribution for all formulations. As shown in Fig. 3, the DOMC7 (a) and DOMC–FA2 (b) self-aggregates in PBS solution (pH 7.4) have a mean diameter of 231 nm and 179 nm, respectively, with a unimodal size distribution. Overall, the sizes of self-aggregates based on DOMCs were larger than those based on DOCA-modified chitosan (161–180 nm) (Lee, Jo, Kwon, Kim, & Jeong, 1998), but smaller than those based on DOCA-modified glycol chitosan (245–450 nm) (Kim et al., 2005). The different solubility among chitosan, OCMC and glycol chitosan should affect the size of self-aggregates. Moreover, the different molecular weight might be another possible reason; for example, the increase in the molecular weight of chitosan was demonstrated to increase the size of self-aggregates because of the rigidity of the chitosan chain (Kim et al., 2001; Kwon et al., 2003). From the data listed above, it was clear that self-aggregates of DOMC–FAs showed slightly smaller size and narrower size distribution than those of DOMC7, which illustrated that FA had a relatively weaker hydrophobicity in the media of PBS solution (pH = 7.4) and might involve in the formation of self-aggregates like DOCA. However, as the DS of FA increased, the size of self-aggregates of DOMC–FA decreased more slowly compared with DOMC which depended on the DS of DOCA. It was indicated that, most of the folic acid were dissolved in the media and on the surface of self-aggregates as a targeting group. This will be confirmed in our future work.

The change of the mean diameter of DOMC7 and DOMC–FA2 self-aggregates as a function of concentration of conjugations in PBS solution (pH = 7.4) were investigated (data not shown). The size of self-aggregates was scarcely affected by the concentration of DOMC7 and DOMC–FA2 in the range of 0.5–5 mg/mL. It is concluded that the interparticle interaction between self-aggregates is almost negligible. Considering the biomedical uses of self-aggregates as a drug delivery system in the body, it is very important that the size of self-aggregates in PBS solution (pH = 7.4) is independent on the concentration of amphiphilic polymers (Lee, Jo, et al., 1998).

The analysis of zeta potential, which was the electric potential at the plane of shear, was a useful tool to predict the physical storage stability of colloidal systems. The nanoparticles had the higher zeta potential value, indicating the better stability of this colloidal system (Teeranachaideekul, Souto, Junyaprasert, & Muller, 2007). In our study, the zeta potential values of all self-aggregates were negative, about −16 mV (Table 1), which indicated that nanoparticles were covered with negatively charged carboxyl groups of OCMC. Also, the absolute value of zeta potential of the self-aggregates decreased in PBS, which might be due to that electrolytes in PBS screen the negative charges in the OCMC backbone (Gao et al., 2008). These results implied that self-aggregates were electrostatically stabilized with negative OCMC shells. In general, the zeta potential values higher than −30 mV signify long-term stability of aqueous dispersion. However, despite a zeta potential below the critical value of −30 mV, nanoparticles can have the same long-term stability, in case the sterical hindrance layer is sufficiently thick (Müller & Jacobs, 2002; Müller, Jacobs, & Kayser, 2001).

Fig. 4 shows the morphology of self-aggregates in the transmission electron microscope photographs. Since all the samples have similar images, the images of DOMC7 (a) and DOMC–FA2 (b) were chosen as sample. TEM observation confirmed that self-aggregates composed nanoparticles with a uniform size distribution and their shapes were near spherical. The mean diameter of self-aggregates appeared to be a little different from the results determined by zetasizer measurement, which could primarily be ascribed to the change of self-aggregates during the drying procedure for the preparation of TEM specimen. Since zetasizer method involves the measurement of size in the hydrated state, whereas TEM images obtain the size at the dried state of the sample. Hence, the size observed by TEM method was smaller than the size measured by zetasizer method. However, the general tendency, depending on the DS, was in a good agreement. A similar finding has been reported by other authors (Jiang, Quan, Liao, & Wang, 2006; Prabha, Zhou, Panyam, & Labhasetwar, 2002).

OCMC, which is a derivative of chitin, was obtained via a carboxymethylation reaction from chitosan. As an amphiphilic

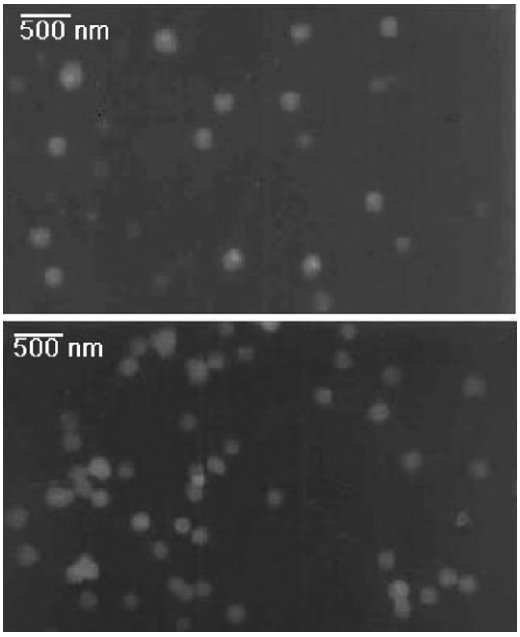

Fig. 4. TEM images of self-aggregates of DOMC7 (a) and DOMC–FA2 (b) (2 mg/mL).

polyelectrolyte, it has weak base cationic ($-NH_3^+$) groups and also contains weak acid anionic ($-COO^-$) groups. The effects of pH of the medium on the aggregation of the modified OCMC are important. As shown in Table 2, the particle size of DOMC7 and DOMC–FA2 changed in PBS solution of different pH values, owing to the protonation of amino groups and deionization of carboxyl groups. The self-aggregates of the modified OCMC in PBS solution at pH 6.8 have a smaller mean diameter than those in PBS solution of other pH values. The possible reason is that the pH 6.8 was close to the isoelectric point of modified OCMC, so, the amino groups were well-protonated and the surface carboxyl groups were deionized in PBS solution of pH 6.8. Consequently, the hydrophobic interaction counteracted the electrostatic repulsion, resulting in the formation of smaller self-aggregates. It is indicated that the modified OCMC had a certain pH sensitivity.

3.3. Critical aggregation concentration of self-aggregates

The aggregation behavior of DOMC and DOMC–FA conjugates in the aqueous media was determined using a probe fluorescence technique in the presence of pyrene as a fluorescence probe. If polymeric micelles are formed in an aqueous solution, pyrene molecules preferably locate inside or close to the hydrophobic micro-domains of micelles rather than the aqueous phase, resulting in different photophysical characteristics (Amiji, 1995; Wilhelm et al., 1991). Therefore, the fluorescence emission spectra of pyrene incorporated into self-aggregates of DOMC and DOMC–FA were obtained

Table 2
Properties of DOCA hydrophobic-modified OCMC and FA conjugations in PBS solutions of different pH.

Sample	pH	d^d (nm)	PI[d]	CAC[f] (mg/mL)
DOMC7	6.0	243.7	0.352	0.0287
	6.8	222.5	0.335	0.0265
	7.4	231.1	0.365	0.0273
DOMC–FA2	6.0	197.2	0.359	0.0241
	6.8	168.9	0.339	0.0215
	7.4	179.4	0.345	0.0227

[d] Mean diameter and polydispersity indices measured by a Zetasizer.
[f] Critical aggregation concentration determined by fluorescence spectroscopy.

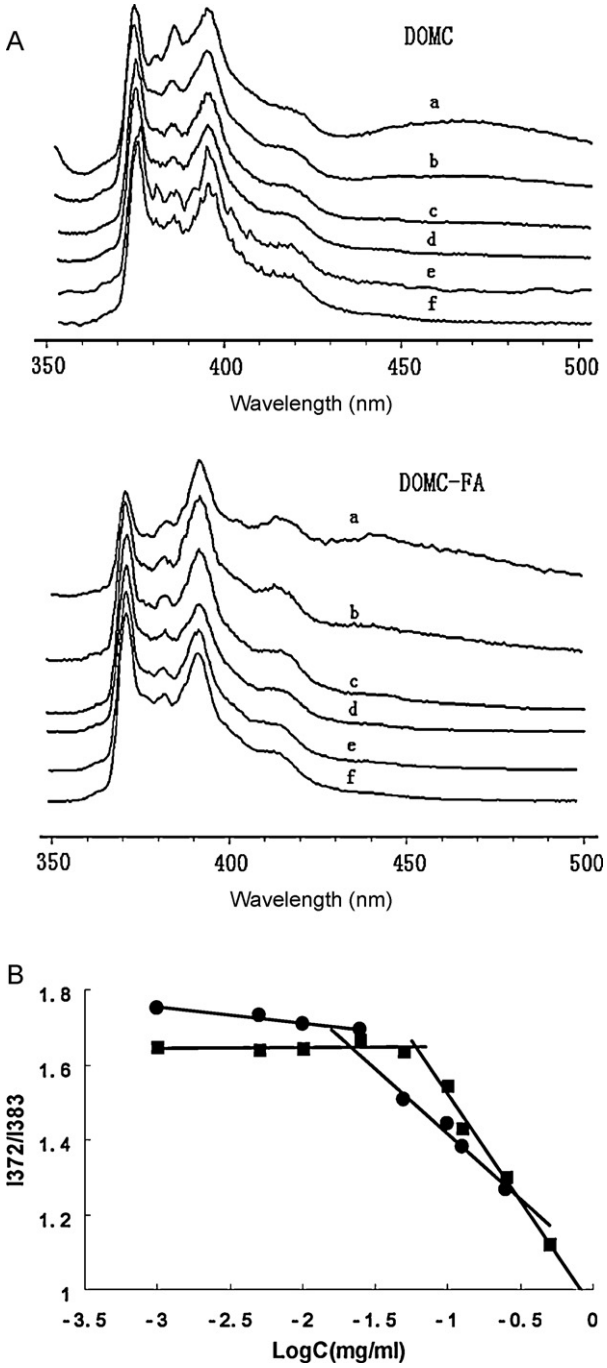

Fig. 5. (A) Excitation spectra of pyrene in PBS solution (pH 7.4) in the presence of DOMC7 and DOMC–FA2 (a) 0.5, (b) 0.25, (c) 0.1, (d) 0.05 (e) 0.01 and (f) 0.001 mg/mL. The excitation wavelength was 334 nm, and the spectra were accumulated with an integration time of 4 s/1 nm. (B) Intensity ratio (I_{372}/I_{383}) from pyrene excitation spectra as a function of polymer concentration in PBS solution (pH 7.4): (■) DOMC7 and (●) DOMC–FA2.

at various concentrations in PBS solution (pH = 7.4), as shown in Fig. 5A (DOMC7 and DOMC–FA2). The total fluorescence intensity showed no significant changes at low concentration ranges of self-aggregates. As the concentration increases, however, the total emission intensity increases and especially the intensity of the third highest vibrational band at 383 nm (I_3) starts to drastically increase at a certain concentration of amphiphilic polymer. This concentration is defined as a critical aggregation concentration (CAC), meaning the threshold concentration of self-aggregates of amphiphilic polymer by intra- or intermolecular association, which

can be determined from the crossover point in the low concentration ranges. Fig. 5B shows the intensity ratio (I_{372}/I_{383}) of the pyrene excitation spectra versus the logarithm of the DOMC7 and DOMC–FA2 concentration. The CAC values of the DOMC conjugates were in the range of 0.027–0.065 mg/mL, which decreased with the increase in the content of hydrophobic DOCA because of enhanced hydrophobicity (Table 1). The CAC values of DOMCs were lower than those of low molecular weight surfactants, e.g., 1.0 mg/mL for DOCA (Kratohvil, Hsu, & Kwok, 1986) and 2.3 mg/mL for sodium dodecyl sulfate in water (Rahman & Brown, 2003), indicating the DOMCs were a novel kind of amphiphilic polymers and could form the stable self-aggregates in a aqueous media. The variation tendency of CAC values with DS of DOMCs is similar to that of DOCA-modified chitosan (DCs) (Lee, Jo, et al., 1998) and DOCA-modified glycol chitosan (GCDs) (Kim et al., 2005), however, the obtained cac values are larger than those of DCs (0.013–0.045 mg/mL) which possess less hydrophobic DOCA. It suggested that the hydrophilic nature of the OCMC backbone in DOMCs hampered significantly the effective association among hydrophobic DOCAs. While, the cac values of the DOMC–FA conjugates were slightly lower those that of DOMC7 (Table 1), which illustrated that FA had a barely hydrophobic interaction in the media of PBS solution (pH = 7.4), meaning that most of the FA were dissolved in the media and on the surface of self-aggregates. Also, the CAC values of DOMC7 and DOMC–FA2 were different in PBS solution of different pH values (Table 2). The CAC values in PBS solution of pH 6.8 were lower than which were in PBS solution of other pH values and the reasons have been explained above. These results are consistent with our previous findings in the particle size study.

4. Conclusion

Novel kinds of amphiphilic polymer, namely, DOCA and FA modified OCMC, were prepared and various physicochemical properties of these self-aggregates in aqueous phases were investigated. The mean diameters of self-aggregates of DOMCs were in the range of 231–383 nm and DOMC–FAs were slightly smaller in the range of 179–212 nm, with a narrow and unimodal size distribution. The critical aggregation concentrations of DOMC conjugates were in the range of 0.027–0.065 mg/mL, and the CAC of DOMC–FA conjugates were slightly lower than that of DOMC7. The mean diameters and the CAC values depended on the DS and changed with the pH value. The size of self-aggregates is independent on the concentration of amphiphilic polymers in physiological conditions. Results demonstrated that self-aggregates with hydrophobic domain and targeted groups on the surface were composed of multiple polymer chains. The study of physicochemical properties suggests the potential applicability of self-aggregates to the pharmaceutical and biomedical fields, especially being used as the delivery of anti-tumor drugs, and the further investigations are in progress.

Acknowledgment

This work was supported by the National Basic Research Program of China (973 Program), No. 2009CB930300.

References

Amiji, M. M. (1995). Pyrene fluorescence study of chitosan self association in aqueous solution. *Carbohydrate Polymers*, *26*, 211–213.

Akiyoshi, K., Deguchi, S., Moriguchi, N., Yamaguchi, S., & Sunamoto, J. (1993). Self-aggregates of hydrophobized polysaccharides in water. Formation and characteristics of nanoparticles. *Macromolecules*, *26*, 3062–3068.

Akiyoshi, K., Kang, E. C., Kurumada, S., Sunamoto, J., Principi, T., & Winnik, F. M. (2000). Controlled association of amphiphilic polymers in water: Thermosensitive nanoparticles formed by self-assembly of hydrophobically modified pullulans and poly(N-isopropylacrylamides). *Macromolecules*, *33*, 3244–3249.

Chan, P., Kurisawa, M., Chung, J. E., & Yang, Y. Y. (2007). Synthesis and characterization of chitosan-g-poly(ethylene glycol)–folate as a non-viral carrier for tumor-targeted gene delivery. *Biomaterials*, *28*, 540–549.

Chen, L. Y., Du, Y. M., Tian, Z. G., & Sun, L. P. (2005). Effect of the degree of deacetylation and the substitution of carboxymethyl chitosan on its aggregation behavior. *Journal of Polymer Science Part B: Polymer Physics*, *43*, 296–305.

Chen, X. G., & Park, H. J. (2003). Chemical characteristics of O-carboxymethyl chitosans related to the preparation conditions. *Carbohydrate Polymers*, *53*, 355–359.

Enhsen, A., Kramer, W., & Wess, G. (1998). Bile acids in drug discovery. *Drug Discovery Today*, *3*, 409–418.

Gao, F. P., Zhang, H. Z., Liu, L. R., Wang, Y. S., Jiang, Q., Yang, X. D., et al. (2008). Preparation and physicochemical characteristics of self-assembled nanoparticles of deoxycholic acid modified-carboxymethyl curdlan conjugates. *Carbohydrate Polymers*, *71*, 606–613.

Gref, R., Minamitake, Y., Peracchia, M. T., Trubetskoy, V., Torchilin, V., & Langer, R. (1994). Biodegradable long-circulating polymeric nanospheres. *Science*, *263*, 1600–1603.

Han, X., Liu, J., Liu, M., Xie, C., Zhan, C. Y., Gu, B., et al. (2009). 9-NC-loaded folate-conjugated polymer micelles as tumor targeted drug delivery system: Preparation and evaluation in vitro. *International Journal of Pharmaceutics*, *372*, 125–131.

Huh, K. M., Lee, K. Y., Kwon, I. C., Kim, Y. H., Kim, C., & Jeong, S. Y. (2000). Synthesis of triarmed poly(ethylene oxide)–deoxycholic acid conjugate and its micellar characteristics. *Langmuir*, *16*, 10566–10568.

Jiang, G. B., Quan, D. P., Liao, K. R., & Wang, H. H. (2006). Preparation of polymeric micelles based on chitosan bearing a small amount of highly hydrophobic groups. *Carbohydrate Polymers*, *66*, 514–520.

Kabanov, A. V., Nazarova, I. R., Astafieva, I. V., Batrakova, E. V., Alakhov, V. Y., Yaroslavov, A. A., et al. (1995). Micelle formation and solubilisation of fluorescent probes in poly(oxyethylene-b-oxyethylene-b-oxyethylene) solutions. *Macromolecules*, *28*, 2303–2314.

Kakizawa, Y., Harada, A., & Kataoka, K. (2001). Glutathione-sensitive stabilization of block copolymer micelles composed of antisense DNA and thiolated poly(ethylene glycol)-block-poly(L-lysine): A potential carrier for systemic delivery of antisense DNA. *Biomacromolecules*, *2*, 491–497.

Kataoka, K., Harada, A., & Nagasaki, Y. (2001). Block copolymer micelles for drug delivery: Design, characterization and biological significance. *Advance Drug Delivery Review*, *47*, 113–131.

Kataoka, K., Kwon, G. S., Yokoyama, M., Okano, T., & Sakurai, Y. (1993). Block copolymer micelles as vehicles for drug delivery. *Journal of Controlled Release*, *24*, 119–132.

Kim, C., Lee, S. C., Kang, S. W., Kwon, I. C., Kim, Y., & Jeong, S. Y. (2000). Synthesis and the micellar characteristics of poly(ethylene oxide)–deoxycholic acid conjugates. *Langmuir*, *16*, 4792–4797.

Kim, C., Lee, S. C., Kwon, I. C., Chung, H., & Jeong, S. Y. (2002). Complexation of poly(2-ethyl-2-oxazoline)-block-poly(ε-carprolactone) micelles with multifunctional carboxylic acids. *Macromolecules*, *35*, 193–200.

Kim, K., Kwon, S., Park, J. H., Chung, H., Jeong, S. Y., & Kwon, I. C. (2005). Physicochemical characterizations of self-assembled nanoparticles of glycol chitosan–deoxycholic acid conjugates. *Biomacromolecules*, *6*, 1154–1158.

Kim, Y. H., Gihm, S. H., Park, C. R., Lee, K. Y., Kim, T. W., Kwon, I. C., et al. (2001). Structural characteristics of size-controlled self-aggregates of de-oxycholic acid-modified chitosan and their application as a DNA delivery carrier. *Bioconjugate Chemistry*, *12*, 932–938.

Koping-Hoggard, M., Tubulekas, I., Guan, H., Edwards, K., Nilsson, M., Varum, K. M., et al. (2001). Chitosan as a nonviral gene delivery system. Structure–property relationships and characteristics compared with polyethylenimine in vitro and after lung administration in vivo. *Gene Therapy*, *8*, 1108–1121.

Kratohvil, J. P., Hsu, W. P., & Kwok, V. (1986). How large are the micelles of di-a-hydroxy bile salts at the critical micellization concentrations in aqueous electrolyte solutions? Results for sodium taurodeoxycholate and sodium deoxycholate. *Langmuir*, *2*, 256–258.

Kuroda, K., Fujimoto, K., Sunamoto, J., & Akiyoshi, K. (2002). Hierarchical self-assembly of hydrophobically modified pullulan in water: Gelation by networks of nanoparticles. *Langmuir*, *18*, 3780–3786.

Kwon, S., Park, J. H., Chung, H., Kwon, I. C., Jeong, S. Y., & Kim, I. (2003). Physicochemical characteristics of self-assembled nanoparticles based on glycol chitosan bearing 5 beta-cholanic acid. *Langmuir*, *19*, 10188–10193.

Lee, E. S., Na, K., & Bae, Y. H. (2003). Polymeric micelle for tumor pH and folate-mediated targeting. *Journal of Controlled Release*, *91*, 103–113.

Lee, K. Y., Kwon, I. C., Kim, Y. H., Jo, W. H., & Jeong, S. Y. (1998). Preparation of chitosan self-aggregates as a gene delivery system. *Journal of Controlled Release*, *51*, 213–220.

Lee, K. Y., Jo, W. H., Kwon, I. C., Kim, Y., & Jeong, S. Y. (1998). Physicochemical characteristics of self-aggregates of hydrophobically modified chitosans. *Langmuir*, *14*, 2329–2332.

Lee, K. Y., Kim, J. H., Kwon, I. C., & Jeong, S. Y. (2000). Selfaggregates of deoxycholic acid-modified chitosan as a novel carrier of adriamycin. *Colloids Polymer Science*, *278*, 1216–1219.

Lee, R. J., & Low, P. S. (1994). Delivery of liposomes into cultured KB cells via folate receptor-mediated endocytosis. *Journal of Biological Chemistry*, *4*, 3198–3204.

Lee, S. C., Chang, Y., Yoon, J.-S., Kim, C., Kwon, I. C., Kim, Y.-H., et al. (1999). Synthesis and micellar characterization of amphiphilic diblock copolymers based on poly (2-ethyl-2-oxazoline) and aliphatic polyesters. *Macromolecules*, *32*, 1847–1852.

Liu, S. Q., Wiradharma, N., Gao, S. J., Tong, Y. W., & Yang, Y. Y. (2007). Bio-functional micelles self-assembled from a folate-conjugated block copolymer for targeted intracellular delivery of anticancer drugs. *Biomaterials*, *28*, 1423–1433.

Liu, X. F., Guan, Y. L., Yang, D. Z., Li, Z., & Yao, K. D. (2001). Antibacterial action of chitosan and carboxymethylated chitosan. *Journal of Applied Polymer Science*, *79*, 1324–1335.

Lu, Y., & Low, P. S. (2003). Immunotherapy of folate receptor-expressing tumors: Review of recent advances and future prospects. *Journal of Controlled Release*, *91*, 17–29.

Mansouri, S., Cuie, Y., Winnik, F., Shi, Q., & Lavigne, P. (2006). Characterization of folate–chitosan–DNA nanoparticles for gene therapy. *Biomaterials*, *27*, 2060–2065.

Mortensen, K. (2001). Structural properties of self-assembled polymeric aggregates in aqueous solutions. *Polymer Advance Technology*, *12*, 2–22.

Müller, R. H., & Jacobs, C. (2002). Buparvaquone mucoadhesive nanosuspension: Preparation, optimisation and long-term stability. *International Journal of Pharmaceutics*, *237*, 151–161.

Müller, R. H., Jacobs, C., & Kayser, O. (2001). Nanosuspensions as particulate drug formulations in therapy: Rationale for development and what we can expect for the future. *Advanced Drug Delivery Reviews*, *47*, 3–19.

Na, K., & Bae, Y. H. (2002). Self-assembled hydrogel nanoparticles responsive to tumor extracellular pH from pullulan derivative/sulfonamide conjugate: Characterization, aggregation, and adriamycin release in vitro. *Pharmaceutical Research*, *19*, 681–688.

Nagasaki, Y., Yasugi, K., Yamamoto, Y., Harada, A., & Kataoka, K. (2001). Sugar-installed block copolymer micelles: Their preparation and specific interaction with lectin molecules. *Biomacromolecules*, *2*, 1067–1070.

Nichifor, M., & Carpov, A. (1999). Bile acids covalently bound topolysaccharides. 1. Esters of bile acids with dextran. *European Polymer Journal*, *35*, 2125–2129.

Oyewumi, M. O., Yokel, R. A., Jay, M., Coakley, T., & Mumper, R. J. (2004). Comparison of cell uptake, biodistribution and tumor retention of folate-coated and PEG-coated gadolinium nanoparticles in tumor-bearing mice. *Journal of Controlled Release*, *95*, 613–626.

Park, E. K, Lee, S. B., & Lee, Y. M. (2005). Preparation and characterization of methoxy poly(ethylene glycol)/poly(e-caprolactone) amphiphilic block copolymeric nanospheres for tumorspecific folate-mediated targeting of anticancer drugs. *Biomaterials*, *26*, 1053–1061.

Park, J. H., Kwon, S., Nam, J., Park, R., Chung, H., Seo, S. B., et al. (2004). Self-assembled nanoparticles based on glycol chitosan bearing 5β-cholanic acid for RGD peptide delivery. *Journal of Controlled Release*, *95*, 579–588.

Poppe, A., Willner, L., Allgaier, J., Stellbrink, J., & Richter, D. (1997). Structural investigation of micelles formed by an amphiphilic PEP–PEO block copolymer in water. *Macromolecules*, *30*, 7462–7471.

Prabha, S., Zhou, W. Z., Panyam, J., & Labhasetwar, V. (2002). Size dependency of nanoparticle-mediated gene transfection: Studies with fractionated nanoparticles. *International Journal Pharmacuetics*, *244*, 105–115.

Rahman, A., & Brown, C. W. (2003). Effect of pH on the critical micelle concentration of sodium dodecyl sulphate. *Journal of Applied Polymer Science*, *28*, 1331–1334.

Reddy, J. A., & Low, P. S. (1998). Folate-mediated targeting of therapeutic and imaging agents to cancers. *Critical Reviews in Therapeutic Drug Carrier Systems*, *15*, 587–627.

Ruel-Gariepy, E., Leclair, G., Hildgen, P., Gupta, A., & Leroux, J. C. (2002). Thermosensitive chitosan-based hydrogel containing liposomes for the delivery of hydrophilic molecules. *Journal of Controlled Release*, *82*, 373–383.

Sandula, J., Kogan, G., Kacurakova, M., & Machova, E. (1999). Microbial (1-3)-b-D-glucans, their preparation, physicochemical characterization and immunomodulatory activity. *Carbohydrate Polymers*, *38*, 247–253.

Son, Y. J., Jang, J., Cho, Y. W., Chung, H., Park, R., Kwon, I. C., et al. (2003). Biodistribution and anti-tumor efficacy of doxorubicin loaded glycol-chitosan nanoaggregates by EPR effect. *Journal of Controlled Release*, *91*, 135–145.

Tae, G., Kornfield, J. A., Hubbell, J. A., & Lal, J. (2002). Ordering transitions of fluoroalkyl-ended poly(ethylene glycol): Rheology and SANS. *Macromolecules*, *35*, 4448–4457.

Teeranachaideekul, V., Souto, E. B., Junyaprasert, V. B., & Muller, R. H. (2007). Cetyl palmitate-based NLC for topical delivery of coenzyme Q10-development, physicochemical characterization and in vitro release studies. *European Journal of Pharmaceutics*, *67*, 141–148.

Tobio, M., Gref, R., Sanchez, A., Langer, R., & Alonso, M. J. (1998). Stealth PLA–PEG nanoparticles as protein carriers for nasal administration. *Pharmaceutical research*, *15*, 270–275.

Wan, A. J., Sun, Y., & Li, H. L. (2008). Characterization of folate-graft-chitosan as a scaffold for nitric oxide release. *International Journal of Biological Macromolecules*, *43*, 415–421.

Wang, S., Luo, J., Lantrip, D. A., Waters, D. J., Mathias, C. J., Green, M. A., et al. (1997). Design and synthesis of [^{111}In] DTPA–folate for use as tumortargeted radiopharmaceutical. *Bioconjugate Chemistry*, *8*, 673–679.

Wilhelm, M, Zhao, C., Wang, Y., Xu, R., Winnik, M. A., Mura, J., et al. (1991). Poly(styrene-ethylene oxide) block copolymer micelle formation in water: A fluorescence probe study. *Macromolecules*, *24*, 1033–1040.

Yang, S. J., Lin, F. H., Tsai, K. C., Wei, M. F., Tsai, H. M., Wong, J. M., et al. (2010). Folic acid-conjugated chitosan nanoparticles enhanced protoporphyrin IX accumulation in colorectal cancer cells. *Bioconjugate Chemistry*, *21*, 679–689.

Yuan, X. B., Li, H., Zhu, X. X., & Woo, H. G. (2006). Self-aggregated nanoparticles composed of periodate-oxidized dextran and cholic acid: Preparation, stabilization and in-vitro drug release. *Journal of Chemical Technology and Biotechnology*, *81*, 746–754.

Yuan, X. B., Li, H., & Yuan, Y. B. (2006). Preparation of cholesterol modified chitosan self-aggregates for delivery of drugs to ocular surface. *Carbohydrate Polymers*, *65*, 337–345.

Zhang, Y., & Zhang, M. (2002). Calcium phosphate/chitosan composite scaffolds for controlled in vitro antibiotic drug release. *Journal of Biomedical Materials Research*, *62*, 378–386.

Zhang, Y., Kohler, N., & Zhang, M. (2002). Surface modification of superparamagnetic magnetite nanoparticles and their intracellular uptake. *Biomaterials*, *23*, 1553–1561.

Zhao, H. Z., Yue, L., & Lanry, Y. (2008). Selectivity of folate conjugated polymer micelles against different tumor cells. *International Journal of Pharmaceutics*, *349*, 256–268.